

# PDE6 in Lamprey *Petromyzon marinus*: Implications for the Evolution of the Visual Effector in Vertebrates<sup>†,‡</sup>

Hakim Muradov, Kimberly K. Boyd, Vasily Kerov, and Nikolai O. Artemyev\*

Department of Molecular Physiology and Biophysics, University of Iowa College of Medicine, Iowa City, Iowa 52242

Received March 16, 2007; Revised Manuscript Received June 28, 2007

**ABSTRACT:** Photoreceptor rod and cone phosphodiesterases comprise the sixth family of cyclic nucleotide phosphodiesterases (PDE6). PDE6s have uniquely evolved as effector enzymes in the vertebrate phototransduction cascade. To understand the evolution of the PDE6 family, we have examined PDE6 in lamprey, an ancient vertebrate group. A single PDE6 catalytic subunit transcript was found in the sea lamprey *Petromyzon marinus* cDNA library. The lamprey PDE6 sequence showed a high degree of homology with mammalian PDE6 and equally distant relationships with the rod and cone enzymes. In contrast, two different PDE6 inhibitory  $P\gamma$  subunits, a cone-type  $P\gamma 1$  and a mixed cone/rod-type  $P\gamma 2$ , have been identified in the lamprey retina. Immunofluorescence analysis demonstrated that  $P\gamma 1$  and  $P\gamma 2$  are expressed in the long and short photoreceptors of sea lamprey, respectively. The catalytic PDE6 subunit was present in the photoreceptors of both types and colocalized with the  $P\gamma$  subunits. Recombinant  $P\gamma 1$  and  $P\gamma 2$  potently inhibited trypsin-activated lamprey and bovine PDE6 enzymes. Our results point to a high degree of conservation of PDE6 genes during the vertebrate evolution. The apparent duplication of the  $P\gamma$  gene in the stem of vertebrate lineage may have been an essential component of the evolution of scotopic vision in early vertebrates.

Cyclic nucleotides phosphodiesterases (PDEs) are essential regulators of cellular levels of cAMP and cGMP. PDEs in vertebrates are classified into 11 families on the basis of sequence homology, substrate selectivity, and regulation (1–3). PDEs within each of the families have 60% or more homology, while similarities between different families are 40% or less. Photoreceptor PDEs are expressed in rod and cone photoreceptor cells and comprise the PDE6<sup>1</sup> family. Rod photoreceptor PDE6 is a heterotetramer containing a catalytic heterodimer of large homologous  $\alpha$ - and  $\beta$ -subunits (PDE6 $\alpha\beta$ ) and two copies of the inhibitory  $\gamma$  subunit ( $P\gamma$ ) (4). Cone PDE is composed of two identical PDE $\alpha'$  subunits each bound to a cone-specific  $P\gamma$  subunit (4). PDE6s are the effector enzymes in the vertebrate phototransduction cascade. In rods, photoexcited rhodopsin activates the rod G protein, transducin, which subsequently stimulates PDE6 by displacing the  $P\gamma$  subunits from PDE $\alpha\beta$  (5–7). A similar cascade in cones involves cone opsins and cone transducin.

In terms of domain structure and sequence homology, PDE6 is most closely related to cGMP-specific PDE5 and dual-substrate PDE11. The phylogenetic analysis of PDEs and the similarities in the exon organization indicate that

PDE6, PDE5, and PDE11 have a common ancestral gene (8). PDE6, PDE5, and PDE11, as well as two other PDE families (PDE2 and PDE10), contain two N-terminal regulatory GAF domains (9, 10). The C-terminal catalytic domains of PDE6, PDE5, and PDE11 share ~45% sequence identity. Functionally, PDE6 is more similar to PDE5, with the two enzymes displaying strong substrate preference for cGMP and common sensitivity to drugs, such as sildenafil (Viagra) and vardenafil (Levitra) (4, 11). Besides PDE5 in vertebrates, PDE5-like genes are readily identifiable in genomes of invertebrate species, including arthropods (*Drosophila melanogaster*), echinoderms (sea urchin *Strongylocentrotus purpuratus*), and tunicates (*Ciona intestinalis*, *Ciona savignyi*) (Supporting Information Figure 2). However, authentic PDE6s are only found in vertebrates. All three PDE6 genes coding rod PDE6 $\alpha\beta$  and cone PDE $\alpha'$  as well as genes for rod and cone  $P\gamma$  subunits are present in bony fishes *Danio rerio* and *Tetraodon nigroviridis*, which are currently the most distant vertebrate species with completed genome sequences.

During evolution and, perhaps, concurrently with the appearance of vertebrate photoreceptors, PDE6 acquired unique properties critical for phototransduction: (a) a tight interaction with  $P\gamma$  that blocks the enzyme catalytic site in the dark and (b) a nearly perfect cGMP-hydrolytic efficiency in the absence of the  $P\gamma$  block that provides for required amplification of the visual signal. By comparison, PDE5 does not interact with  $P\gamma$ , and its catalytic rate constant for cGMP hydrolysis is almost 1000-fold lower than that of activated PDE6 (4, 12). Not only is it unknown how these unique properties of PDE6 have evolved, but the underlying structural determinants also remain obscure, in part because

<sup>†</sup> This work was supported by National Institutes of Health Grant EY10843.

<sup>‡</sup> The nucleotide sequences reported in this paper have been submitted to the GenBank with accession numbers EF427669, EF432251, and EF470978.

\* To whom correspondence should be addressed. Phone: (319) 335-7864. Fax: (319) 335-7330. E-mail: nikolai-artemyev@uiowa.edu.

<sup>1</sup> Abbreviations: PDE6, cone or rod outer segment cGMP phosphodiesterase; lamPDE6, PDE6 from sea lamprey *Petromyzon marinus*;  $P\gamma$ , inhibitory subunit of PDE6;  $P\gamma 1$  and  $P\gamma 2$ ,  $P\gamma$  subunits from sea lamprey *P. marinus*; ROS (OS), rod outer segment.

an expression system for PDE6 is lacking (13–15). Unlike PDE6, functional PDE5 is expressed with ease in various systems (16–18). PDE6 enzymes in early vertebrates may structurally be more similar to the ancestral enzyme and be more amenable to heterologous expression than mammalian PDE6. Thus, cloning and characterization of PDE6 from ancient vertebrate species provides an opportunity to investigate the evolution of PDE6 and, potentially, to gain insights into the enzyme structure–function relationships.

Hagfish and lampreys are the only surviving representatives of the earliest known vertebrate class of jawless fish. They evolved in the lower Cambrian period 540 million years ago (19). Hagfishes are traditionally linked with vertebrates even though they never replace their notochord with a vertebral column. The eyes in hagfish may have undergone a degenerative evolution and are very primitive pitlike structures often lacking a cornea, lens, and vitreous body (20). In contrast, lampreys possess fully structured eyes with a differentiated retina and well-characterized photoreceptor cells (21). We chose to clone PDE6 from the northern hemisphere sea lamprey *Petromyzon marinus*, which has previously served as an evolutionary model for various organs and systems, including vision (21, 22).

## EXPERIMENTAL PROCEDURES

**Materials.** The Novagen OrientExpress cDNA Library Construction  $\lambda$ SCREEN kit was from Novagen. [ $^3\text{H}$ ]cGMP was a product of Amersham Pharmacia Biotech (GE Healthcare). All restriction enzymes were purchased from NEB. AmpliTaq DNA polymerase was a product of Applied Biosystems, and Pfu DNA polymerase was a product of Stratagene. SulfoLink gel was a product of Pierce. All other reagents were purchased from Sigma.

**Lamprey Retina cDNA Libraries.** Heads of sea lamprey *P. marinus* were frozen on dry ice immediately after decapitation and shipped from the Hammond Bay Biological Station (U.S. Geological Survey, Millersburg, MI). The eyeballs were removed from slightly thawed lamprey heads, and the retinas were quickly dissected and homogenized in the TRI reagent (Molecular Research Center, Cincinnati, OH) using 1 mL of the reagent/100 mg of retina. The total retinal RNA was isolated using the manufacturer's protocol. An MRC oligo(dT) column was used to isolate poly(A)RNA. The total RNA and poly(A)RNA were utilized immediately or stored at  $-80^\circ\text{C}$ . The first strand of cDNA was synthesized by oligo(dT) priming of the total retina RNA or by random priming (TTNNNNNN) of poly(A)RNA. A Novagen OrientExpress cDNA Library Construction  $\lambda$ SCREEN kit was used to synthesize double-stranded cDNA and to generate the  $\lambda$  phage library. cDNA was first ligated to directional linkers containing *Eco*RI and *Hind*III sites and then cloned into the bacteriophage  $\lambda$  vector  $\lambda$ SCREEN-1. Following in vitro packaging, the phages were mixed with the host strain ER1647 and plated according to the manufacturer's protocol. The phage library size was estimated at  $1.4 \times 10^6$  pfu. The phage library DNA was isolated from phage lysate according to a published protocol (23). To obtain bacterial cDNA libraries, an equal portion of the linker-flanked lamprey retinal cDNA was ligated into the pCR2.1 vector (Invitrogen) using the *Eco*RI/*Hind*III sites.

**Lamprey PDE6 Cloning.** Six forward and reverse degenerated oligonucleotide primers corresponding to highly con-

served sequences within the PDE5/6/11 catalytic domains were used in various combinations to amplify the lamprey's retinal cDNA. PCR amplification using a forward primer, AAGGGCTACAGAGACATCACCTACCATAACTGGMGRCAYGGSTTYAAY (PDE6 sequence KGYRDITYHNWRHGFN), paired with the reverse primer CTGGACTTCCCATGGCTTGTAATGGCAGACAAGTCACATCCHGTCATCAT (PDE6 sequence MMTGCDLSAITKPWEVQ) yielded a product corresponding to an appropriate portion of PDE6 ORF as confirmed by DNA sequencing. On the basis of this PDE6 sequence, a radioactive [ $^{32}\text{P}$ ]DNA probe was synthesized by random priming of the PCR product template corresponding to residues 569–694 of the full-length lamprey PDE6 with the use of the Klenow fragment of *Escherichia coli* DNA polymerase I. The probe was hybridized to the bacterial oligo(dT) cDNA library in aqueous solution (0.5 mM NaHPO<sub>4</sub>, pH 7.2, 1% BSA, 1 mM Na<sub>2</sub>EDTA, 7% SDS) overnight at  $65^\circ\text{C}$  and washed five times using low-stringency wash buffer (40 mM NaHPO<sub>4</sub>, pH 7.2, 0.5% BSA, 1 mM Na<sub>2</sub>EDTA, 5% SDS) at  $25^\circ\text{C}$ . A total of 16 positive colonies were identified. The DNA sequencing revealed that all 16 insert DNAs were of insignificantly varying lengths and covered the catalytic domain and the 3' untranslated region of the same PDE6 DNA. We were unable to obtain the N-terminal PDE6 sequence by screening the bacterial oligo(dT) or the  $\lambda$  phage cDNA libraries. Screening of the random priming-generated cDNA library with a [ $^{32}\text{P}$ ]DNA probe corresponding to residues 491–539 of the full-length catalytic subunit produced five positive colonies with inserts covering the 5' untranslated region and the N-terminal PDE6 DNA sequence overlapping with the catalytic domain sequence.

To clone the  $\text{P}\gamma$  subunit(s) of PDE6, lamprey retinal cDNA was used as the template in PCR amplification with a degenerative forward primer, ACYMGNCARTTCAAGAG (aa T[S/R]QFKS), and a degenerative reverse primer, CCRWAYTGRGCMARYTCGTG (aa HE[L/F]AQ[Y/F]G). A primer corresponding to the conserved  $\text{P}\gamma$  region, MEGLGTDITVICPW, was synthesized on the basis of the sequence of the PCR product obtained using the degenerate primers above. This primer was paired with a  $\lambda$ SCREEN-1-specific primer for PCR amplification using the  $\lambda$  phage library DNA as the template. The products of this amplification were cloned into the pCR2.1 vector, transformed into TOP10 *E. coli* cells, and plated according to the TA cloning kit manual (Invitrogen). Analysis of plasmids from 25 colonies showed the presence of DNA inserts coding for two different  $\text{P}\gamma$  subunits,  $\text{P}\gamma 1$  (18 colonies) and  $\text{P}\gamma 2$  (7 colonies).  $\text{P}\gamma 1$ - and  $\text{P}\gamma 2$ -specific [ $^{32}\text{P}$ ]DNA probes were synthesized by random priming using the corresponding plasmid DNA inserts. Screening of the random priming-generated cDNA library with [ $^{32}\text{P}$ ]DNA probes identified colonies containing the full-length ORF for  $\text{P}\gamma 1$ , but not  $\text{P}\gamma 2$ . The missing C-terminal sequence of  $\text{P}\gamma 2$  was identified by sequencing PCR products obtained with amplification of the  $\lambda$  phage library DNA using a  $\lambda$ SCREEN-1-specific primer and a  $\text{P}\gamma 2$ -specific primer corresponding to  $\text{P}\gamma 2$  residues 1–10.

**Expression of the Lamprey PDE6 Catalytic Domain and  $\text{P}\gamma$  Subunits in *E. coli*.** The DNA sequence for the catalytic domain lampPDE6(480–814) was amplified using lamprey retina cDNA as the template and primers containing *Spe*I (forward primer) and *Bam*HI (reverse primer) sites and

subcloned into the modified pET15b vector. The lamPDE6-(480–814) expression was induced at temperatures ranging from 12 to 37 °C, and the recombinant protein was isolated as previously described (24). DNA sequences coding the P $\gamma$ 1 and P $\gamma$ 2 subunits (P $\gamma$ 2(1–89) and P $\gamma$ 2(13–89)) were amplified from lamprey retinal cDNA using primers containing *Xho*I (forward primers) and *Bam*HI (reverse primers) sites and subcloned into the pET15b vector using *Xho*I and *Bam*HI restriction enzymes. The sequences of all constructs were verified by automated DNA sequencing at the University of Iowa DNA Core Facility. The single-colony cultures were incubated overnight at 37 °C and diluted to 0.5–1.0 L (1:100) with 2xTY medium containing ampicillin. Cell cultures with OD = 1.0 were induced at 25 °C with the addition of 0.5 mM IPTG. After 4 h of incubation, the cells were pelleted and stored at –80 °C. The recombinant P $\gamma$  subunits were purified using His-bind resin (Novagen) (24) and reversed-phase chromatography on a C4 column (25). The His-tag was cleaved off the P $\gamma$  polypeptides using thrombin.

**Partial Purification of PDE6 from Lamprey Retinas.** A total of 20 retinas were removed from partially thawed lamprey eyeballs and homogenized with a Pyrex glass pestle tissue grinder in 2.5 mL of 10 mM Tris–HCl buffer (pH 7.5) containing 2 mM  $\beta$ -mercaptoethanol and 1 mM MgSO<sub>4</sub> (buffer A). The supernatant (20 min, 21000g) was saved, and the pellet was additionally extracted two times with buffer A using the above procedure. The three supernatants were combined, centrifuged (100000g, 40 min), and applied to a 0.5 mL DEAE column equilibrated with buffer A. The column was washed with buffer A, and the proteins were eluted with 100, 200, 300, and 400 mM NaCl steps in buffer A. Fractions containing PDE6 activity were eluted with 200 mM NaCl. Partially purified PDE6 preparations were stored at –20 °C with the addition of 40% glycerol. Trysin-activated lamprey PDE6 and purified trypsin-activated bovine rod PDE6 were obtained as described (25).

**Antibodies.** Rabbit polyclonal antibodies have been custom-made by Sigma-Genosys against the following peptides: lamPDE6(14–27), DSNPNFAQEYFNRKC; lamPDE6(687–701), ETLGNEAEAIKYITC; P $\gamma$ 1(2–15), SEKTSNTLAPVPTH; P $\gamma$ 2(2–15), NLATANTSGALMAPC; P $\gamma$ 2(7–20), CNTSGALMAPTKVSG. The peptides were conjugated to keyhole limpet hemocyanin via the terminal Cys residues. The lamprey PDE6 subunit-specific antibodies were immunoaffinity-purified on peptide-SulfoLink resins. Rabbit sera were loaded onto the columns with 1 mL of peptide-SulfoLink gel equilibrated with PBS. The antibodies were eluted with 50 mM glycine–HCl (pH 2.5) and immediately dialyzed against 50 mM HEPES/Na (pH 7.5) solution containing 200 mM NaCl. Anti-P $\gamma$ (63–87) antibody was a gift of Dr. R. Cote (University of New Hampshire). Polyclonal anti-His6 antibodies were from Santa Cruz.

**Immunofluorescence.** Lamprey eyeballs were enucleated, poked through the cornea with a 21-gauge needle, and fixed in 4% formaldehyde in phosphate-buffered saline for 2 h at 25 °C. After fixation, the eyeballs were cut in half, the cornea and lens were removed, and the eyecups were submersed in a 30% sucrose solution in phosphate-buffered saline for 5 h at 4 °C. The eyecups were then embedded in tissue freezing medium (TBS) and frozen on dry ice. Radial sectioning

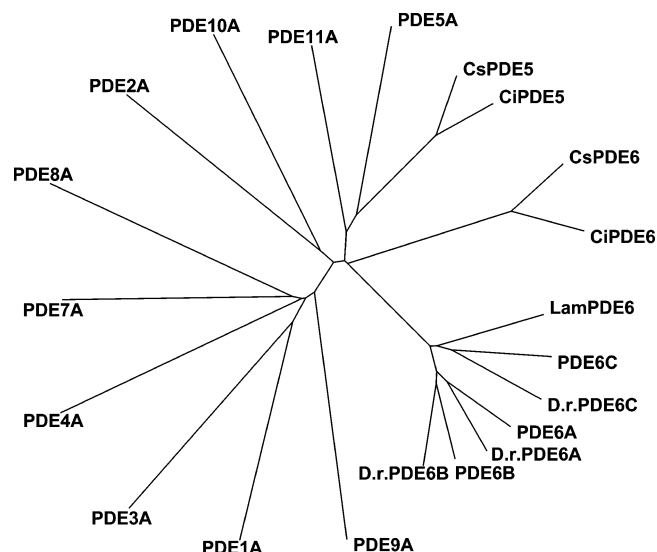


FIGURE 1: Phylogenetic tree of PDE families. The tree was generated by the neighbor-joining method using a multiple alignment of the full-length protein sequences and the Gonnet 250 matrix at the EBI ClustalW Web server. The alignment included lamPDE6 and human PDEs: PDE1A (P54750), PDE2A (O00410), PDE3A (Q14432), PDE4A (P27815), PDE5A (O76074), PDE6A (P16499), PDE6B (P35913), PDE6C (P51160), PDE7A (Q13946), PDE8A (O60658), PDE9A (O76083), PDE10A (Q9Y233), PDE11 (Q9HCR9). The zebrafish *Danio rerio* PDE6s were added to the alignment to augment the PDE6 branch (D.r. PDE6A (NP\_001007161), D.r. PDE6B (XP\_685002), D.r. PDE6C (NP\_957165)). CsPDE6 (gene ID ENSCSAVG 00000010358, translation ID ENSCSAVP 00000017594) and CiPDE6 (scaffold\_55, SNAP\_CIONA 0000003-6352) are divergent PDE6-like PDEs in *C. savignyi* and *C. intestinalis*, respectively. *C. savignyi* CsPDE5 (gene ID ENSCSAVG 00000005480) and *C. intestinalis* CiPDE5 (gene ID ENSCING 00000003569) were included in the alignment to illustrate that the tunicates possess both PDE6- and PDE5-like enzymes.

(10  $\mu$ m) of the retina was performed using a cryomicrotome, Microm HM 505E. Retinal cryosections were air-dried and kept at –80 °C until use. Before staining, sections were warmed to 25 °C and incubated in 0.1% Triton/phosphate-buffered saline for 30 min followed by incubation with 2% normal goat serum/5% bovine serum albumin in phosphate-buffered saline for 30 min. Rabbit P $\gamma$ 1 (1:1000), P $\gamma$ 2 (1:1000), and lamPDE6 (1:1000) antibodies were used. Sections were incubated with primary antibody for 3 h followed by a 1 h incubation with goat anti-rabbit AlexaFluor 546 secondary antibodies (Molecular Probes) (1:1000). For double staining, sections then were incubated with goat anti-rabbit Fab fragments (1:20) for 1 h to block the remaining free epitopes of primary antibodies. After this, sections were stained with other primary rabbit antibody (3 h) followed by a 1 h incubation with anti-rabbit secondary antibody conjugated with AlexaFluor 488. Staining was visualized using a Zeiss LSM 510 confocal microscope.

**Other Methods.** Western blot analysis of lamprey PDE6 subunits was performed following SDS–PAGE in 10% gels using rabbit PDE6- and P $\gamma$ -specific antibodies, anti-rabbit antibodies conjugated to horseradish peroxidase (Sigma), and an ECL reagent (Amersham Biosciences). PDE activity was measured using 200  $\mu$ M [<sup>3</sup>H]cGMP, and the *K<sub>i</sub>* values for inhibition by the P $\gamma$ 1 and P $\gamma$ 2 subunits were determined as described (24).



## A

Pγ1	MS--EK--TSNTLAPPVTHTGPTTPKKGPPKFKQRA	TRQF	FKSKPPKPGVK	KGFGDE	IPGMEGLGTDITV	ICPWEAF	SHLELHEL	AQYGI	V	85					
cGal.g.	MS--EN--PTTNLTGDAPTGPTTPRKGP	PKFKQRT	RQF	FKSKPPKKG	VKGFGDD	IPGMEGLGTDITV	ICPWEAF	SHLELHEL	AQFGI	I	85				
cHum	MS--DN--TT--LPAPASNQSGPTTPRKGP	PKFKQRT	RQF	FKSKPPKKG	VKGFGDD	IPGMEGLGTDITV	ICPWEAF	SHLELHEL	AQFGI	I	83				
cBov	MS--DN--TV--LAPPTSNQSGPTTPRKGP	PKFKQRT	RQF	FKSKPPKKG	VKGFGDD	IPGMEGLGTDITV	ICPWEAF	SHLELHEL	AQFGI	I	83				
cMus	MS--DS--PS--LSPAPSQSGPTTPRKGP	PKFKQRT	RQF	FKSKPPKKG	VKGFGDD	IPGMEGLGTDITV	ICPWEAF	SHLELHEL	AQFGI	I	83				
cXen.t.	MNSGSP--ASSALAPVNNSSGGPTTPRKGP	PKFKQRT	RQF	FKSKPPKKG	VKGFGDD	IPGMEGLGTDITV	ICPWEAF	SHLELHEL	AQFGI	I	87				
cXen.l.	MNGNSP--ASSALAPVNNSSGGPTTPRKGP	PKFKQRT	RQF	FKSKPPKKG	VKGFGDD	IPGMEGLGTDITV	ICPWEAF	NHLELHEL	AQFGI	I	87				
cRana	MNSSSP--AASALALGNVQGGPTTPRKGP	PKFKQRT	RQF	FKSKPPKKG	VKGFGDD	IPGMEGLGTDITV	ICPWEAF	SHLELHEL	AQFGI	I	87				
rXen.t.	MNLEPA--KAEIKSATRV	TGGPAT	PRKGP	PKFKQRT	RQF	FKSKPPKKG	VKGFGDD	IPGMEGLGTDITV	ICPWEAF	NHLELHEL	AQYGI	I	87		
rXen.l.	MNLEPA--KPEIKSATRV	TGGPAT	PRKGP	PKFKQRT	RQF	FKSKPPKKG	VKGFGDD	IPGMEGLGTDITV	ICPWEAF	NHLELHEL	AQYGI	I	87		
rD.r.	MNLEPP--KPEIKSATRV	TGGPAT	PRKGP	PKFKQRT	RQF	FKSKPPKKG	VKGFGDD	IPGMEGLGTDITV	ICPWEAF	NHLELHEL	AQYGI	I	87		
rRana	MNLEPA--KPDIKSATRV	TGGPAT	PRKGP	PKFKQRT	RQF	FKSKPPKKG	VKGFGDD	IPGMEGLGTDITV	ICPWEAF	NHLELHEL	AQYGI	I	87		
rGal.g.	MSLEPH--KPEIKSATRV	TGGPAT	PRKGP	PKFKQRT	RQF	FKSKPPKKG	VKGFGDD	IPGMEGLGTDITV	ICPWEAF	SHLELHEL	AQYGI	I	87		
rBov	MNLEPP--KAEIKSATRV	TGGPAT	PRKGP	PKFKQRT	RQF	FKSKPPKKG	VKGFGDD	IPGMEGLGTDITV	ICPWEAF	NHLELHEL	AQYGI	I	87		
rHum	MNLEPP--KAEIKSATRV	TGGPAT	PRKGP	PKFKQRT	RQF	FKSKPPKKG	VKGFGDD	IPGMEGLGTDITV	ICPWEAF	NHLELHEL	AQYGI	I	87		
rMus	MNLEPP--KGEIKSATRV	TGGPAT	PRKGP	PKFKQRT	RQF	FKSKPPKKG	VKGFGDD	IPGMEGLGTDITV	ICPWEAF	NHLELHEL	AQYGI	I	87		
rTuk.r.	MNLEP---KAEIKSATRV	TGGPAT	PRKGP	PKFKQRT	RQF	FKSKPPKKG	VKGFGDD	IPGMEGLGTDITV	ICPWEAF	NHLELHEL	AQYGI	I	86		
rTet.n.	MNLEP---KAEIKSATRV	TGGPAT	PRKGP	PKFKQRT	RQF	FKSKPPKKG	VKGFGDD	IPGMEGLGTDITV	ICPWEAF	SHLELHEL	AQYGI	I	86		
Pγ2	MNLA	TANTSGAL	MAPTKVSGG	PATPRG	SKFKQRT	RQF	FKSKPPKKG	VKGFGDD	IPGMEGLGTDITV	ICPWEAF	NHLELHEL	AQYGI	L	89	
cTet.n.	MNANPP---	AGSAL	APGGST	GPTTPKKG	PPKFKQRT	RTF	FKSKAPK	PGQK	KGFGDD	IPGMEGLGTDITV	VCPWEAF	GDMELSDL	AKYGI	I	86
cD.r.	MDVAEP---	VE-----	KRG	GPPKFKQRT	TRTF	FKSKAPK	PGQK	KGFGDD	IPGMEGLGTDITV	ICPWEAF	GDMELSDL	AKYGI	L	73	
cTuk.r.	MNASPP---	AGSAL	APGGAT	GPTTPKKG	PPKFKQRT	RTF	FKSKAPK	PGQK	KGFGDD	IPGMEGLGTDITV	VCPWEAF	GDMELSDL	AKYGI	I	86

## B

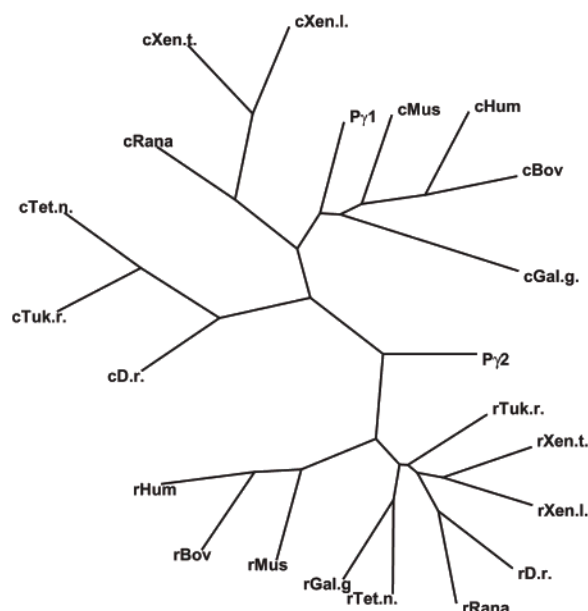


FIGURE 2: (A) Sequence alignment of lamprey's P $\gamma$ 1 and P $\gamma$ 2 with P $\gamma$  subunits from various vertebrate species. ClustalW multiple alignment of cone P $\gamma$  subunits (cHum, human Q13956; cBov, bovine P22571; cMus, murine NP\_076387; cGal.g, chicken AAO67734; cRana, *Rana pipiens* AAK95403; cXen.t., *Xenopus tropicalis* NP\_001016745; cXen.l., *Xenopus laevis* AAH74358; cD.r., *D. rerio* NP\_957079; cTet.n., *Tetraodon nigroviridis* CAF95021; cTuk.r., *Takifugu rubripes* IMCB peptide ID NEWSINFRUP 00000130651) and rod P $\gamma$  subunits (rHum, human P18545; rBov, bovine P04972; rMus, murine P09174; rGal.g, chicken NP\_989776; rRana, *R. pipiens* AAK95404; rXen.t., *X. tropicalis* Ensembl peptide ID ENSXETP 00000054098; rXen.l., *X. laevis* AAH74367; rD.r., *D. rerio* NP\_997964; rTet.n., *T. nigroviridis* CAG03058; rTuk.r., *T. rubripes* IMCB peptide ID NEWSINFRUP 00000163566). (B) A phylogenetic tree of P $\gamma$  subunits was obtained on the basis of a ClustalW multiple alignment of the full-length protein sequences. The consensus tree was produced using a PHYLIP-NEIGHBOR program with a bootstrapping protocol (199 replicates) in a neighbor-joining format through the Web-based Max-Planck Institute's Bioinformatics Toolkit. The sequences in the alignment were the following: (cone P $\gamma$  subunits) cHum, human Q13956; cBov, bovine P22571; cMus, murine NP\_076387; cGal.g, chicken AAO67734; cRana, *R. pipiens* AAK95403; cXen.t., *X. tropicalis* NP\_001016745; cXen.l., *X. laevis* AAH74358; cD.r., *D. rerio* NP\_957079; cTet.n., *T. nigroviridis* CAF95021; cTuk.r., *T. rubripes* IMCB peptide ID NEWSINFRUP 00000130651; (rod P $\gamma$  subunits) rHum, human P18545; rBov, bovine P04972; rMus, murine P09174; rGal.g, chicken NP\_989776; rRana, *R. pipiens* AAK95404; rXen.t., *X. tropicalis* Ensembl peptide ID ENSXETP 00000054098; rXen.l., *X. laevis* AAH74367; rD.r., *D. rerio* NP\_997964; rTet.n., *T. nigroviridis* CAG03058; rTuk.r., *T. rubripes* IMCB peptide ID NEWSINFRUP 00000163566.

## RESULTS

**Identification and Characterization of the Lamprey PDE6 Catalytic Subunit.** To identify and characterize lamprey PDE6, we first created a cDNA library by oligo(dT) priming of the retinal RNA from lamprey *P. marinus*. This library was screened with DNA probes produced by PCR amplification of lamprey cDNA using degenerate primers corresponding to the catalytic domain sequences that are highly

conserved among PDE5/6/11. The screening of  $3 \times 10^5$  colonies yielded 16 independent clones each containing partial sequences corresponding to the same PDE6 catalytic domain. The catalytic domain sequence was used to obtain clones containing the full-length PDE6 catalytic subunit from the random priming-generated cDNA library.

An alignment of the deduced lamprey PDE6 (lamPDE6) sequence with the sequences of human PDE6  $\alpha$ ,  $\beta$ , and  $\alpha'$

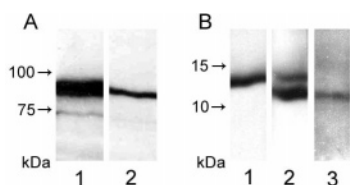


**FIGURE 3:** Expression of lampPDE6, P $\gamma$ 1, and P $\gamma$ 2 in the lamprey's retina. The samples of lamprey retinal homogenates (40  $\mu$ g of protein each) were subjected to 10% Laemmli SDS-PAGE for separation of high molecular weight proteins (A) or to 10% Tris-tricine SDS-PAGE for separation of P $\gamma$  subunits (B) and analyzed by Western blotting using immunoaffinity-purified anti-lampPDE6-(14–27) and anti-lampPDE6(687–701) antibodies (A, lanes 1 and 2, respectively) and anti-P $\gamma$ 1(2–15), anti-P $\gamma$ (63–87), and anti-P $\gamma$ 2-(7–20) (B, lanes 1, 2, and 3, respectively). For accurate identification of the protein positions detected with different antibodies, the lamprey retinal homogenates were loaded into a single 20 mm width well. After separation and transfer of the proteins onto a nitrocellulose membrane, it was stained with Ponceau S to visualize the lanes, and each lane was cut into 5–7 mm vertical strips for further antibody staining.

subunits shows a remarkable degree of conservation, particularly within the catalytic and GAF domains (Supporting Information Figure 1). Similarly to other PDE6s, the C-terminus of lampPDE6 contains the CAAX box, a motif for isoprenylation. The Prenylation Prediction Suite predicts that the C-terminal CVIV sequence in lampPDE6 is farnesylated (26). Interestingly, lampPDE6 is almost equally distantly related to cone and rod PDE6. LampPDE6 is 67% identical to both human PDE6 $\alpha'$  and human PDE6 $\beta$  and 66% identical to human PDE6 $\alpha$ . The phylogenetic analysis of PDEs indicates that lampPDE6 diverged at a time close to duplication of a common cone/rod ancestral PDE6 gene (Figure 1, Supporting Information Figure 2).

The failure of functional expression of mammalian PDE6 has been linked to the folding defects of the catalytic domain (12, 24). To explore the possibility that the catalytic domain

of lampPDE6 would be amenable to expression in *E. coli*, it was subcloned into the pET15b vector. The sequence for the lampPDE6 construct, lampPDE(480–814), was selected to align exactly with the catalytic construct of PDE5 that is readily expressed in *E. coli* and crystallized (18, 27). The recombinant lampPDE6 catalytic domain was found predominantly in insoluble inclusion bodies. Trace amounts of the PDE6 proteins detected in the supernatant by Western blotting did not show enzymatic activity (not shown).

**Inhibitory P $\gamma$  Subunits in Sea Lamprey Retina.** PCR amplifications of the retinal phage library DNA with P $\gamma$ -sequence-directed primers and screening of the bacterial cDNA library with P $\gamma$  DNA probes allowed identification and sequencing of two different P $\gamma$  subunits in lamprey retina, P $\gamma$ 1 and P $\gamma$ 2. Sequence alignment of P $\gamma$ 1 and P $\gamma$ 2 with the rod and cone P $\gamma$  subunits from higher vertebrates demonstrates a strong homology throughout the molecules, except for the 20 aa residue N-terminal segments (Figure 2A). This sequence alignment was used to generate a P $\gamma$  phylogenetic tree (Figure 2B). The P $\gamma$  tree shows a relatively compact branch for rod P $\gamma$  subunits and a looser branch for cone P $\gamma$  subunits. The phylogenetic analysis places P $\gamma$ 1 in the cone group, while P $\gamma$ 2 occupies a transitional cone-to-rod branch (Figure 2B).

**Retinal Expression and Cellular Localization of lampPDE6, P $\gamma$ 1, and P $\gamma$ 2.** To determine protein expression and cellular localization of lampPDE6 in the lamprey retina, two antibodies were developed against the N-terminal peptide lampPDE6-(14–27) and peptide lampPDE6(687–701) corresponding to a nonconserved “hairpin” loop within the catalytic domain. Both antibodies recognized a band of  $\sim$ 90 kDa in immunoblots of lamprey's retinal extracts (Figure 3A). The P $\gamma$ 1- and P $\gamma$ 2-specific antibodies were raised against peptides P $\gamma$ 1(2–15), P $\gamma$ 2(2–15), and P $\gamma$ 2(7–20). In addition, an antibody against the bovine rod P $\gamma$  C-terminal peptide

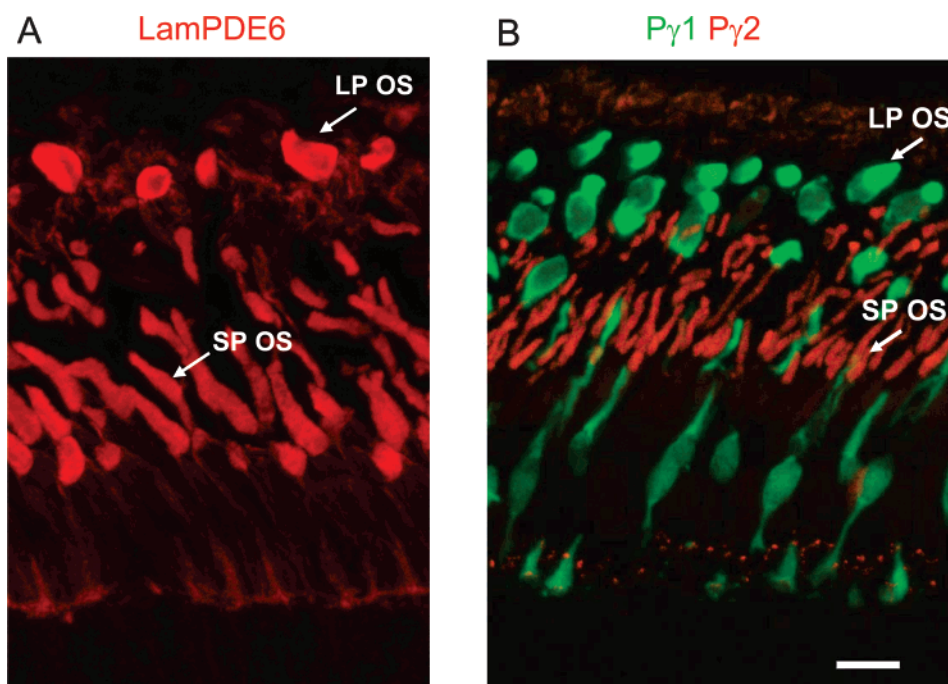


**FIGURE 4:** Localization of lampPDE6, P $\gamma$ 1, and P $\gamma$ 2 in the lamprey's retina. Cryosections of the lamprey retinas were stained with rabbit lampPDE6(14–27) antibody (A) or doubly stained with P $\gamma$ 1(2–15) and P $\gamma$ 2(7–20) antibodies (B) and visualized with goat anti-rabbit AlexaFluor 568 and AlexaFluor 488 secondary antibodies using a Zeiss LSM 510 confocal microscope. Key: P $\gamma$ 1, green; P $\gamma$ 2, red. Abbreviations: LP OS, outer segment of the LP; SP OS, outer segment of the SP. Bar = 10  $\mu$ m.



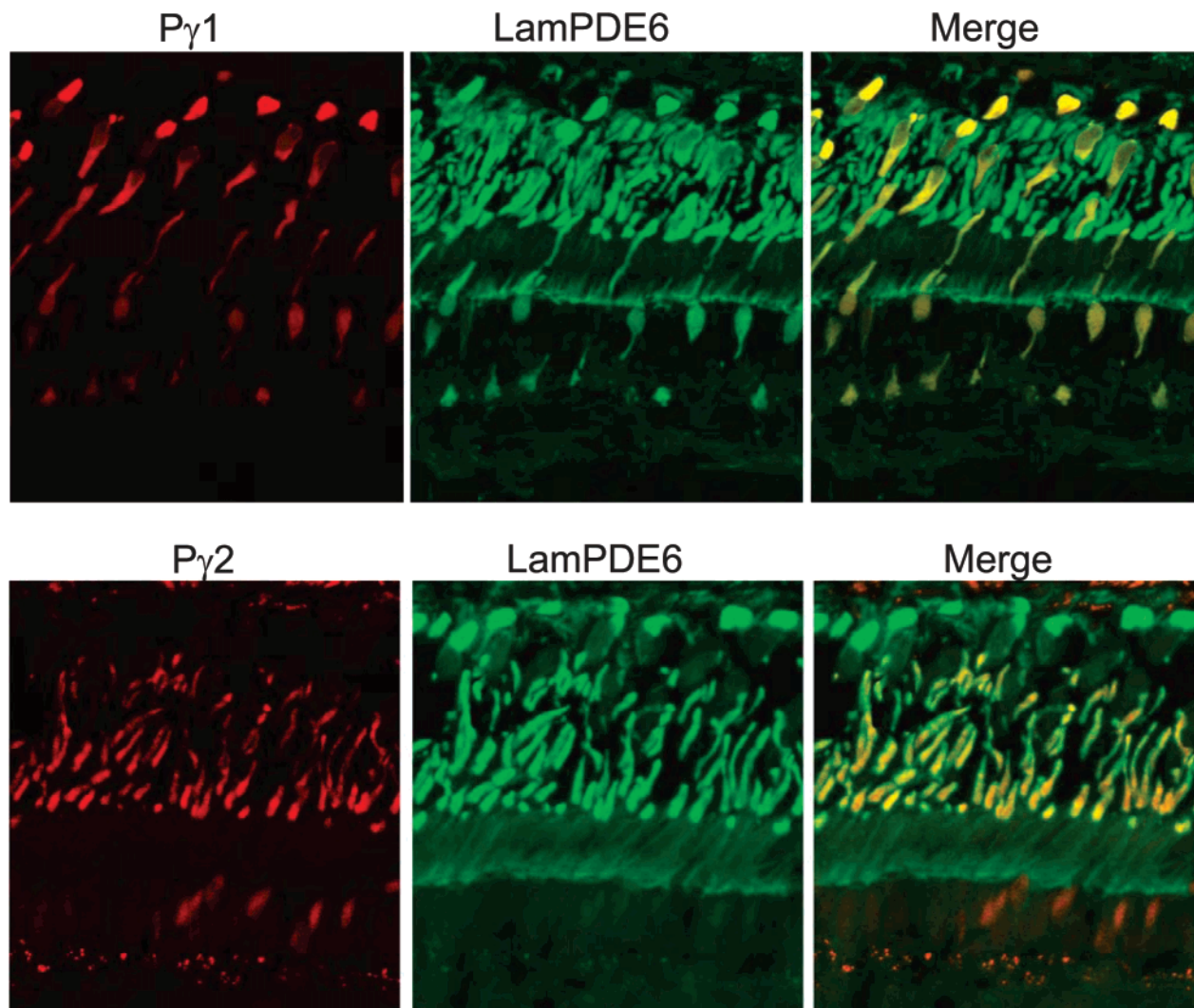


FIGURE 5: Colocalization of lampPDE6 with P $\gamma$ 1 and P $\gamma$ 2. Cryosections of the lamprey retinas were doubly stained with lampPDE6(14–27) antibody and P $\gamma$ 1(2–15) (top panel) or P $\gamma$ 2(7–20) (bottom panel) antibody and visualized with goat anti-rabbit AlexaFluor 568 and AlexaFluor 488 secondary antibodies. LampPDE6 colocalizes with P $\gamma$ 1 in LPs and P $\gamma$ 2 in SPs. Bar = 10  $\mu$ m.

P $\gamma$ (63–87) was utilized. This antibody is predicted to recognize both P $\gamma$ 1 and P $\gamma$ 2. Indeed, P $\gamma$ (63–87) antibody recognized two bands in the lamprey retina extract migrating at  $\sim$ 13 and 11 kDa (Figure 3B). The 13 kDa band also reacted with P $\gamma$ 1(2–15) antibody, whereas the 11 kDa band reacted with P $\gamma$ 2(7–20) antibody. Thus, lampPDE6, P $\gamma$ 1, and P $\gamma$ 2 proteins are expressed in *P. marinus* retina. Noticeably, a predicted 89-residue P $\gamma$ 2 (Figure 2A) migrated on a gel faster than an 85-residue P $\gamma$ 1. In addition, despite an equally good recognition of the recombinant P $\gamma$ 1 and P $\gamma$ 2 proteins by the respective antibodies (not shown), the immunoblot signal in the retinal extracts using the P $\gamma$ 2(7–20) antibody was weaker than that with the P $\gamma$ 1(2–15) antibody (Figure 3B). Contrary to this observation, P $\gamma$ 2 is more abundant in the lamprey retina than P $\gamma$ 1 as seen with P $\gamma$ (63–87) antibodies. A translation of P $\gamma$ 2 from Met13 rather than Met1 (Figure 2A) in the lamprey's retina can explain both the protein's higher gel mobility and reduced P $\gamma$ 2(7–20) antibody recognition. Supporting the translation of P $\gamma$ 2 from Met13, a different P $\gamma$ 2 antiserum, anti-P $\gamma$ 2(2–15), effectively recognized recombinant P $\gamma$ 2, but failed to produce any immunoblot signal using lamprey retina samples (not shown). Furthermore, immunoblot analysis demonstrated that the recombinant P $\gamma$ 2(13–89) and the P $\gamma$ 2 polypeptide in the

lamprey's retina have identical mobility, thus confirming Met13 as a translation initiation site (not shown).

Two morphologically distinct types of photoreceptor cells are described in the sea lamprey retina, short (SPs) and long (LPs) photoreceptors. The more numerous SPs have slender outer segments, while the outer segments of LPs are conical in shape. Elongated myoid regions of LPs join the outer segment to the cell body and extend the LP layer beyond the SP layer (21). Thus, LPs and SPs appear under the microscope as two layers (21, 28). Immunofluorescence staining of the retina sections with lampPDE6(14–27) antibody demonstrated that lampPDE6 is present in the outer segments of both types of photoreceptors (Figure 4A). Immunofluorescence labeling with P $\gamma$ 1(2–15) and P $\gamma$ 2(7–20) antibodies showed that P $\gamma$ 1 is expressed in LPs while P $\gamma$ 2 is localized to the outer segments (OS) of SPs (Figure 4B). In addition to strong OS staining, a weaker P $\gamma$ 1 signal is seen in the long and slender myoid regions connecting the cell bodies of LPs with the OS. Double immunofluorescence labeling indicated that lampPDE6 is colocalized with P $\gamma$ 1 in LPs and with P $\gamma$ 2 in SPs (Figure 5).

**Inhibitory Properties of P $\gamma$ 1 and P $\gamma$ 2.** The cDNAs for P $\gamma$ 1 and P $\gamma$ 2 were subcloned into the pET15b vector, and the P $\gamma$ 1 and P $\gamma$ 2 proteins were expressed in *E. coli* and

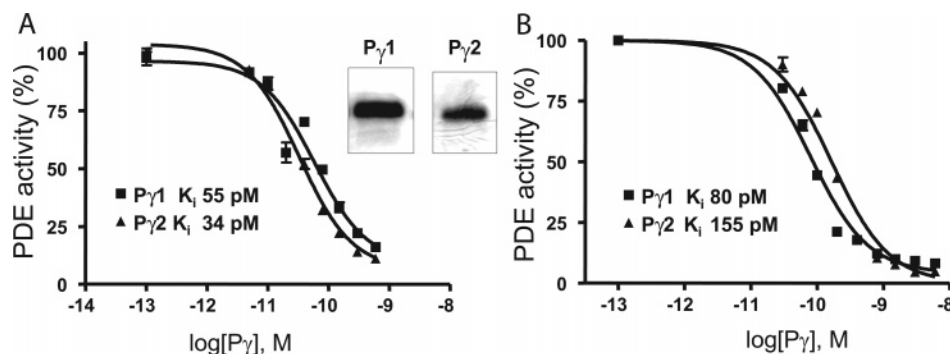


FIGURE 6: Inhibition of PDE6 by P $\gamma$ 1 and P $\gamma$ 2. The activities of trypsin-activated bovine rod PDE6 (A) and lamprey's PDE6 (B) were measured in the presence of 200  $\mu$ M cGMP and increasing concentrations of purified recombinant P $\gamma$ 1 or P $\gamma$ 2 and are expressed as a percentage of the respective PDE activity in the absence of P $\gamma$ . The results of representative experiments are shown. Inset: Coomassie-stained gel of purified P $\gamma$ 1 and P $\gamma$ 2.

purified (Figure 6, inset). First, the ability of P $\gamma$ 1 and P $\gamma$ 2 to inhibit PDE6 was examined using purified bovine rod PDE6 that was treated with trypsin to remove endogenous P $\gamma$ . The trypsin-activated PDE6 was inhibited by P $\gamma$ 2 with a K<sub>i</sub> of 34 pM, while P $\gamma$ 1 was slightly less effective (K<sub>i</sub> of 55 pM) (Figure 6A). The K<sub>i</sub> values for both P $\gamma$ 1 and P $\gamma$ 2 are within the range of K<sub>i</sub> values (10–80 pM) reported for bovine rod P $\gamma$  (29, 30). The inhibition of lampPDE6 by P $\gamma$ 1 and P $\gamma$ 2 was tested using preparations of the enzyme partially purified from lamprey retina extracts and pretreated with trypsin. The trypsin treatment markedly activated lampPDE6 activity, which can be suppressed by the addition of P $\gamma$ 1 or P $\gamma$ 2 (Figure 6B). P $\gamma$ 1 was somewhat more potent in inhibition of lampPDE6 (K<sub>i</sub> of 80 pM) than P $\gamma$ 2 (IC<sub>50</sub> 155 pM). A short form of P $\gamma$ 2, P $\gamma$ 2(13–89), was indistinguishable from the full-length protein in all PDE6 inhibition tests (not shown).

## DISCUSSION

The origins and evolution of PDE6 are poorly understood. Even more obscure is the emergence of the inhibitory P $\gamma$  subunit for PDE6, which had to coevolve with PDE6 for the vertebrate phototransduction cascade to become operational. To explore the evolutionary relationships and characterize PDE6 in ancient vertebrate species, we have cloned PDE6 and the P $\gamma$  subunits from sea lamprey *P. marinus*. A single lamprey PDE6 catalytic subunit transcript and a single corresponding protein product, lampPDE6, were identified in the lamprey's retina. The sequence of lampPDE6 reveals two interesting features: a very high degree of homology to PDE6 from higher vertebrates and its equally distant relationship to cone and rod PDE6. The catalytic domain of lampPDE6 is 80% identical (88% similar) to the catalytic domain of human cone PDE6 $\alpha'$ , underscoring strong conservation of PDE6 during evolution. Therefore, it is not surprising that our attempt to express the lampPDE6 catalytic domain as a functional enzyme was unsuccessful. The phylogenetic analysis indicates that lampPDE6 diverged near the point of duplication of a common cone/rod ancestral PDE6 gene (Figure 1), suggesting that a common ancestor of lamprey and jawed vertebrates possessed one or two genes coding PDE6 catalytic subunit(s). A second PDE6 gene may have been lost in the lamprey branch or converted into a pseudogene. However, a distinct possibility is that lampPDE6 diverged from a single common cone/rod ancestral PDE6.

The evolutionary tree suggests that an ancestral PDE6 gene arose through duplications of a common PDE5/6/11 ancestral gene. Potentially interesting clues to the evolution of PDE6 are provided by the recently sequenced genomes of tunicates *C. savignyi* and *C. intestinalis*. The BLAST search using the Ensemble genome browser identifies 9 PDEs in *C. savignyi*, one of which is grouped with the PDE6 family (csPDE6) (Gene ID ENSCSAVG00000010358, translation IDs ENSCSAVP00000017592 and ENSCSAVP00000017594) (Figure 1). A PDE6-like PDE highly homologous to csPDE6 can also be found in *C. intestinalis* (ciPDE6) (scaffold\_55, SNAP\_CIONA 00000036352) (Figure 1). csPDE6 and ciPDE6 share more than 80% overall identity and more than 90% identity of the catalytic domains. Although csPDE6 and ciPDE6 branch out very early and are highly diverged from vertebrate PDE6s (Figure 1), these are, to our knowledge, the only currently available invertebrate sequences that group together with PDE6s. The properties of *Ciona* PDE6s and vertebrate PDE6s are likely to be very different, and the function of the enzyme in tunicates is unknown. Nonetheless, the csPDE6 and ciPDE6 sequences provide a hint that an ancestral PDE6 may have first appeared in the last common ancestor of urochordates (tunicates) and vertebrates more than 550 million years ago (31). Interestingly, a recent phylogenetic study of 146 nuclear genes from 14 deuterostomes and an out-group of 24 other species presented evidence that tunicates, and not cephalochordates, are the closest living relatives of vertebrates (32). Furthermore, the *Ciona* larvae possess an eyespot (ocellus), which is responsible for the larval light-dependent swimming behavior (33). In the ocellus photoreceptor cells, light activates a phototransduction cascade that shares some striking similarities with the phototransduction pathway in vertebrate photoreceptors (33). It is tantalizing to speculate that the *Ciona* PDE6-like enzymes are involved in the ocellus phototransduction.

The branching of PDE6 appears to have occurred earlier than the divergence of PDE5 and PDE11 (Figure 1, Supporting Information Figure 2). This seems to contradict the fact that PDE6s are only found in vertebrates (and divergent PDE6-like genes in tunicates) while PDE5/11-like genes are also present in echinoderms and arthropods (Supporting Information Figure 2). It is possible, but not likely, that an ancestral PDE6 gene was lost in most invertebrate species. Alternatively, PDE6 may have diverged after separation of PDE5 (or PDE11). The high conservation between lampPDE6



and mammalian PDE6s points to a rapid evolution of PDE6 from an ancestral enzyme prior to the last common ancestor of higher vertebrates and jawless fish. A phylogenetic reconstruction of fast-evolving sequences is pronged to a long-branch attraction artifact (34, 35). This artifact would result in the misplacement of the rapidly evolved PDE6 toward the base of the PDE tree.

In contrast to a single lamPDE6 catalytic subunit, two different P $\gamma$  subunits, P $\gamma$ 1 and P $\gamma$ 2, are identified in the sea lamprey. Except for the short N-terminal segments, P $\gamma$ 1 and P $\gamma$ 2 are highly conserved with the P $\gamma$  subunits from higher vertebrates. The regions of highest conservation in the P $\gamma$  subunits include known interaction sites with the PDE6 catalytic subunits and transducin- $\alpha$  (36, 37). The phylogenetic analysis categorizes P $\gamma$ 1 as a cone-type P $\gamma$  and P $\gamma$ 2 as a mixed cone/rod-type P $\gamma$ . In this respect it is worthy of note that P $\gamma$ 2 was slightly more potent than P $\gamma$ 1 in inhibiting bovine rod PDE6 whereas P $\gamma$ 1 was the more effective of the two P $\gamma$  subunits toward a more ancient lamPDE6. The duplication of the P $\gamma$  gene may have occurred independently in the lamprey branch, but it appears likely that the last common ancestor of lampreys and jawed vertebrates already possessed two P $\gamma$  genes. To date, the genomes of *C. intestinalis*, *C. savignyi*, and lower species provide no indication of the presence of P $\gamma$  genes. In all probability, an ancestral P $\gamma$  gene had evolved and duplicated in the stem of vertebrate lineage.

The P $\gamma$ 1 and P $\gamma$ 2 subunits are expressed in the LP and SP receptor cells, respectively. The nature of these two distinct types of photoreceptor cells in the lamprey retina remains controversial (21, 28, 38, 39). Conflicting morphological, microspectrophotometric, and electrophysiological studies classified both LPs and SPs as cones (21) and rods (38) or LPs as cones and SPs as rods (28, 39). Furthermore, the debate continues on the nature of the visual pigment isolated from *P. marinus*. This pigment was originally considered as an Rh1-like opsin, indicative of the rod photoreceptor function (22). An opposing view is that the lamprey opsin gene evolved prior to duplication of the ancestral Rh gene, which would be consistent with the pigment expression in cones (40, 41). The molecular characteristics and the pattern of expression of lamPDE6 and the P $\gamma$  subunits in the LPs and SPs lend support to the notion that LPs are cones while SPs are mixed cone/rod photoreceptors. In accord, the electroretinographic analysis of the river lamprey *Lampetra fluviatilis* demonstrated that the SPs, similarly to rods, are highly sensitive and can function at scotopic levels of illumination (39), yet SPs do not saturate at high levels of illumination and contribute to photopic cone-mediated vision as well (39). Thus, the physiology of SPs in lamprey appears to reflect the evolution of scotopic vision in early vertebrates, and the duplication of the ancestral P $\gamma$  gene may represent an essential component of this evolution.

## SUPPORTING INFORMATION AVAILABLE

Figures showing the sequence alignment of LamPDE6 and human PDE6 and the phylogenetic tree of PDE families with augmented branches for PDE5, PDE6, and PDE11. This material is available free of charge via the Internet at <http://pubs.acs.org>.

## REFERENCES

- Bender, A. T., and Beavo, J. A. (2006) Cyclic nucleotide phosphodiesterases: molecular regulation to clinical use, *Pharmacol. Rev.* 58, 488–520.
- Francis, S. H., Turko, I. V., and Corbin, J. D. (2001) Cyclic nucleotide phosphodiesterases: relating structure and function, *Prog. Nucleic Acid Res. Mol. Biol.* 65, 1–52.
- Lugnier, C. (2006) Cyclic nucleotide phosphodiesterase (PDE) superfamily: a new target for the development of specific therapeutic agents, *Pharmacol. Ther.* 109, 366–398.
- Cote, R. H. (2004) Characteristics of photoreceptor PDE (PDE6): similarities and differences to PDE5, *Int. J. Impot. Res.* 16, Suppl. 1, S28–33.
- Chabre, M., and Deterre, P. (1989) Molecular mechanism of visual transduction, *Eur. J. Biochem.* 179, 255–266.
- Yarfitz, S., and Hurley, J. B. (1994) Transduction mechanisms of vertebrate and invertebrate photoreceptors, *J. Biol. Chem.* 269, 14329–14332.
- Arshavsky, V. Y., Lamb, T. D., and Pugh, E. N., Jr. (2002) G proteins and phototransduction, *Annu. Rev. Physiol.* 64, 153–187.
- Yuasa, K., Kanoh, Y., Okumura, K., and Omori, K. (2001) Genomic organization of the human phosphodiesterase PDE11A gene. Evolutionary relatedness with other PDEs containing GAF domains, *Eur. J. Biochem.* 268, 168–178.
- Aravind, L., and Ponting, C. P. (1997) The GAF domain: an evolutionary link between diverse phototransducing proteins, *Trends Biochem. Sci.* 22, 458–459.
- Zoraghi, R., Corbin, J. D., and Francis, S. H. (2004) Properties and functions of GAF domains in cyclic nucleotide phosphodiesterases and other proteins, *Mol. Pharmacol.* 65, 267–278.
- Zhang, X., Feng, Q., and Cote, R. H. (2005) Efficacy and selectivity of phosphodiesterase-targeted drugs in inhibiting photoreceptor phosphodiesterase (PDE6) in retinal photoreceptors, *Invest. Ophthalmol. Visual Sci.* 46, 3060–3066.
- Granovsky, A. E., and Artemyev, N. O. (2001) Partial reconstitution of photoreceptor cGMP phosphodiesterase characteristics in cGMP phosphodiesterase-5, *J. Biol. Chem.* 276, 21698–21703.
- Piriev, N. I., Yamashita, C., Samuel, G., and Farber, D. (1993) Rod photoreceptor cGMP-phosphodiesterase: analysis of  $\alpha$  and  $\beta$  subunits expressed in human kidney cells, *Proc. Natl. Acad. Sci. U.S.A.* 90, 9340–9344.
- Qin, N., and Baehr, W. (1994) Expression and mutagenesis of mouse rod photoreceptor cGMP phosphodiesterase, *J. Biol. Chem.* 269, 3265–3271.
- Granovsky, A. E., Natochin, M., McEntaffer, R. L., Haik, T. L., Francis, S. H., Corbin, D. J., and Artemyev, N. O. (1998) Probing domain functions of chimeric PDE6 $\alpha$ /PDE5 cGMP-phosphodiesterase, *J. Biol. Chem.* 273, 24485–24490.
- Turko, I. V., Francis, S. H., and Corbin, J. D. (1998) Hydropathic analysis and mutagenesis of the catalytic domain of the cGMP-binding cGMP-specific phosphodiesterase (PDE5). cGMP versus cAMP substrate selectivity, *Biochemistry* 37, 4200–4205.
- Fink, T. L., Francis, S. H., Beasley, A., and Grimes, K. A., and Corbin, J. D. (1999) Expression of an active, monomeric catalytic domain of the cGMP-binding cGMP-specific phosphodiesterase (PDE5), *J. Biol. Chem.* 274, 34613–34620.
- Sung, B. J., Hwang, K. Y., Jeon, Y. H., Lee, J. I., Heo, Y. S., Kim, J. H., Moon, J., Yoon, J. M., Hyun, Y. L., Kim, E., Eum, S. J., Park, S. Y., Lee, J. O., Lee, T. G., Ro, S., and Cho, J. M. (2003) Structure of the catalytic domain of human phosphodiesterase 5 with bound drug molecules, *Nature* 425, 98–102.
- Xian-guang, H., Aldridge, R. J., Siveter, D. J., Siveter, D. J., and Xiang-hong, F. (2002) New evidence on the anatomy and phylogeny of the earliest vertebrates, *Proc. Biol. Sci.* 269, 1865–1869.
- Fernholm, B., and Holmberg, K. (1975) The eyes in three genera of hagfish (Eptatretus, Paramyxine and Myxine): a case of degenerative evolution, *Vision Res.* 15, 253–259.
- Dickson, D. H., and Graves, D. A. (1979) Fine structure of the lamprey photoreceptors and retinal pigment epithelium (*Petromyzon marinus* L.), *Exp. Eye Res.* 29, 45–60.
- Zhang, H., and Yokoyama, S. (1997) Molecular evolution of the rhodopsin gene of marine lamprey, *Petromyzon marinus*, *Gene* 191, 1–6.
- Benson, S., and Taylor, R. K. (1984) A rapid small-scale procedure for isolation of phage  $\lambda$  DNA, *Biotechniques* 2, 126–127.



24. Muradov, K. G., Boyd, K. K., and Artemyev, N. O. (2006) Analysis of PDE6 function using chimeric PDE5/6 catalytic domains, *Vision Res.* 46, 860–868.
25. Artemyev, N. O., Natochin, M., Busman, M., Schey, K. L., and Hamm, H. E. (1996) Mechanism of photoreceptor PDE inhibition by its  $\gamma$ -subunits, *Proc. Natl. Acad. Sci. U.S.A.* 93, 5407–5412.
26. Maurer-Stroh, S., and Eisenhaber, F. (2005) Refinement and prediction of protein prenylation motifs, *Genome Biol.* 6, R55.
27. Huai, Q., Liu, Y., Francis, S. H., Corbin, J. D., and Ke, H. (2004) Crystal structures of phosphodiesterases 4 and 5 in complex with inhibitor 3-isobutyl-1-methylxanthine suggest a conformation determinant of inhibitor selectivity, *J. Biol. Chem.* 279, 13095–13101.
28. Ishikawa, M., Takao, M., Washioka, H., Tokunaga, F., Watanabe, H., and Tonosaki, A. (1987) Demonstration of rod and cone photoreceptors in the lamprey retina by freeze-replication and immunofluorescence, *Cell Tissue Res.* 249, 241–246.
29. Wensel, T. G., and Stryer, L. (1986) Reciprocal control of retinal rod cyclic GMP phosphodiesterase by its  $\gamma$  subunit and transducin, *Proteins* 1, 90–99.
30. Hamilton, S. E., Prusti, R. K., Bentley, J. K., Beavo, J. A., and Hurley, J. B. (1993) Affinities of bovine photoreceptor cGMP phosphodiesterases for rod and cone inhibitory subunits, *FEBS Lett.* 318, 157–161.
31. Dehal, P., et al. (2002) The draft genome of *Ciona intestinalis*: insights into chordate and vertebrate origins, *Science* 298, 2157–2167.
32. Delsuc, F., Brinkmann, H., Chourrout, D., and Philippe, H. (2006) Tunicates and not cephalochordates are the closest living relatives of vertebrates, *Nature* 439, 965–968.
33. Kusakabe, T., and Tsuda, M. (2006) Photoreceptive Systems in Ascidians. *Photochem. Photobiol.* (in press).
34. Felsenstein, J. (1978) Cases in which parsimony or compatibility methods will be positively misleading, *Syst. Zool.* 27, 401–410.
35. Moreira, D., and Philippe, H. (2000) Molecular phylogeny: pitfalls and progress, *Int. Microbiol.* 3, 9–16.
36. Guo, L. W., Muradov, H., Hajipour, A. R., Sievert, M. K., Artemyev, N. O., and Ruoho, A. E. (2006) The inhibitory  $\gamma$  subunit of the rod cGMP phosphodiesterase binds the catalytic subunits in an extended linear structure, *J. Biol. Chem.* 281, 15412–15422.
37. Slep, K. C., Kercher, M. A., He, W., Cowan, C. W., Wensel, T. G., and Sigler, P. B. (2001) Structural determinants for regulation of phosphodiesterase by a G protein at 2.0 Å, *Nature* 409, 1071–1077.
38. Ohman, P. (1976) Fine structure of the optic nerve of *Lampetra fluviatilis* (Cyclostomi), *Vision Res.* 16, 659–662.
39. Govardovskii, V. I., and Lychakov, D. V. (1984) Visual cells and visual pigments of the lamprey, *Lampetra fluviatilis*, *J. Comp. Physiol.* 154, 279–286.
40. Collin, S. P., Knight, M. A., Davies, W. L., Potter, I. C., Hunt, D. M., and Trezise, A. E. (2003) Ancient colour vision: multiple opsin genes in the ancestral vertebrates, *Curr. Biol.* 13, R864–865.
41. Collin, S. P., and Trezise, A. E. (2004) The origins of color vision in vertebrates, *Clin. Exp. Optom.* 87, 217–223.

BI700535S